Ca^{2+}-induced Ca^{2+} Release in Chinese Hamster Ovary (CHO) Cells Co-expressing Dihydropyridine and Ryanodine Receptors

Norio Suda,* Dorothee Franzius,* Andrea Fleig,* Seiichiro Nishimura,‡ Matthias Bödding,* Markus Hoth,* Hiroshi Takeshima,§ and Reinhold Penner*

From the *Department of Membrane Biophysics, Max-Planck-Institut für biophysikalische Chemie, Am Fassberg, 37077 Göttingen, Germany; ‡Department of Medical Chemistry and Molecular Genetics, Kyoto University Faculty of Medicine, Kyoto 606, Japan; and §Department of Pharmacology, Faculty of Medicine, University of Tokyo, Tokoyo 113, Japan

ABSTRACT Combined patch-clamp and Fura-2 measurements were performed on chinese hamster ovary (CHO) cells co-expressing two channel proteins involved in skeletal muscle excitation-contraction (E-C) coupling, the ryanodine receptor (RyR)-Ca^{2+} release channel (in the membrane of internal Ca^{2+} stores) and the dihydropyridine receptor (DHPR)-Ca^{2+} channel (in the plasma membrane). To ensure expression of functional L-type Ca^{2+} channels, we expressed α_2, β, and γ DHPR subunits and a chimeric DHPR α_1 subunit in which the putative cytoplasmic loop between repeats II and III is of skeletal origin and the remainder is cardiac. There was no clear indication of skeletal-type coupling between the DHPR and the RyR; depolarization failed to induce a Ca^{2+} transient (CaT) in the absence of extracellular Ca^{2+} ($[Ca^{2+}]_o$). However, in the presence of $[Ca^{2+}]_o$, depolarization evoked CaTs with a bell-shaped voltage dependence. About 30% of the cells tested exhibited two kinetic components: a fast transient increase in intracellular Ca^{2+} concentration ($[Ca^{2+}]_i$) (the first component; reaching 95% of its peak <0.6 s after depolarization) followed by a second increase in $[Ca^{2+}]_i$ which lasted for 5–10 s (the second component). Our results suggest that the first component primarily reflected Ca^{2+} influx through Ca^{2+} channels, whereas the second component resulted from Ca^{2+} release through the RyR expressed in the membrane of internal Ca^{2+} stores. However, the onset and the rate of Ca^{2+} release appeared to be much slower than in native cardiac myocytes, despite a similar activation rate of Ca^{2+} current. These results suggest that the skeletal muscle RyR isoform supports Ca^{2+}-induced Ca^{2+} release but that the distance between the DHPRs and the RyRs is, on average, much larger in the cotransfected CHO cells than in cardiac myocytes. We conclude that morphological properties of T-tubules and/or proteins other than the DHPR and the RyR are required for functional "close coupling" like that observed in skeletal or cardiac muscle. Nevertheless, some of our results imply that these two channels are potentially able to directly interact with each other.

KEY WORDS: skeletal muscle • excitation-contraction coupling • cardiac muscle • Fura-2 • voltage-operated Ca^{2+} release

INTRODUCTION

The dihydropyridine receptor (DHPR)[1] and the ryanodine receptor (RyR) are the major proteins thought to be involved in the initial step of excitation-contraction (E-C) coupling, the process that links depolarization of the transverse (T)-tubular membranes to release of Ca^{2+} from the sarcoplasmic reticulum (SR). The DHPRs are located in the T-tubular membranes and are structurally identified as tetrads; the RyRs are located in the SR membranes and are structurally identified as the so-called "feet" which span the gap between the T-tubule and SR membranes (for current reviews see Rios and Pizarro, 1991; Franzini-Armstrong and Jorgensen, 1994; Meissner, 1994).

In skeletal muscle, the DHPRs are considered to primarily function as voltage sensors (Rios and Brum, 1987; Tanabe et al., 1988) for inducing SR Ca^{2+} release possibly via a direct interaction with the RyR-Ca^{2+} release channels (Takeshima et al., 1994; Nakai et al., 1996). Consistent with this is the presence of intramembrane charge movement (Chandler et al., 1976), which indicates molecular rearrangement of the DHPRs (Rios and Brum, 1987; Adams et al., 1990). The voltage sensor hypothesis would account for the following functional features of skeletal muscle (Rios and Pizarro, 1991): (*a*) voltage-gated Ca^{2+} release starts to occur without requiring a second messenger, such as

Address reprint requests to R. Penner, Department of Membrane Biophysics, Max-Planck-Institut fur biophysikalische, Am Fassberg, 37077 Gottingen, Germany. Fax: 49-551-201-1688.

Dr. N. Suda's present address is Department of Anatomy and Neurobiology, Colorado State University, Fort Collins, CO 80523.

Dr. M. Hoth's present address is Department of Molecular and Cellular Physiology, Stanford University, Stanford, CA 94305-5426.

Dr. S. Nishimura's present address is Department of Molecular and Cellular Biology, Nippon Boehringer Ingelheim Co., LTD., Kawanishi Pharma Research Institute, Yato, Takada 103, Kawanishi, Hyogo 666-01, Japan.

[1]*Abbreviations used in this paper:* CaT, Ca^{2+} transient; CHO, Chinese hamster ovary; CICR, Ca^{2+}-induced Ca^{2+} release; CaTR, calcium-transient ratio; DHPR, dihydropyridine receptor; E-C, excitation-contraction; RyR, ryanodine receptor; SR, sarcoplasmic reticulum, T, transverse.

Ca^{2+} or $InsP_3$; (*b*) Ca^{2+} transients (CaTs) exhibit a sigmoidal voltage dependence; and (*c*) Ca^{2+} release flux that occurs following depolarization starts to decay within a millisecond of fiber repolarization. Thus, it is generally believed that the voltage sensors (DHPRs) are mechanically linked to the release channels (RyRs) (Chandler et al., 1976; Rios et al., 1993), a notion strongly supported by ultrastructural evidence (Block et al., 1988) as well as biochemical evidence (Brandt et al., 1990; Marty et al., 1994).

In cardiac myocytes, the DHPR represents a major pathway for entry of extracellular Ca^{2+}, which in turn causes Ca^{2+} release from the SR via the Ca^{2+}-induced Ca^{2+} release (CICR) mechanism (Fabiato, 1985; Beuckelman and Wier, 1988; Näbauer et al., 1989, Cleemann and Morad, 1991). In contrast to skeletal E-C coupling, Ca^{2+} release through the RyRs in cardiac muscle appears to be tightly controlled by both the amplitude and duration of Ca^{2+} current (Cannell et al., 1987; Barcenas-Ruiz and Wier, 1987; Callewaert et al., 1988; Cleemann and Morad, 1991; Wier et al., 1994). Although this behavior is not easily reconciled with the regenerative nature of CICR, it does support the notion that Ca^{2+} release is triggered by Ca^{2+} entry through the Ca^{2+} channels. A recent study using confocal microscopy has demonstrated that Ca^{2+} release occurs within a few milliseconds of depolarization both at the edge and at the deep myoplasm (Cheng et al., 1994). This together with biochemical data (Brandt and Basset, 1986) suggests that a large fraction of the DHPRs reside in the T-tubule membranes, and thereby allow efficacious communication with the RyRs. Consistent with this, a local increase in cytoplasmic free calcium concentration ($[Ca^{2+}]_i$) due to Ca^{2+} entry through the DHPR-Ca^{2+} channels is much more effective in inducing SR Ca^{2+} release than the spatially averaged (global) increase in $[Ca^{2+}]_i$ induced by Ca^{2+} entry through the Na-Ca exchanger (Sham et al., 1995*a*; Lopez-Lopez et al., 1995). Furthermore, Lopez-Lopez et al. (1995) and Cannell et al. (1995) have suggested, again based on confocal microscopy data, that even a single Ca^{2+} channel can induce local Ca^{2+} release from one or a small group of RyRs (Ca^{2+} release element) in a stochastic manner, despite the rather small conductance of the Ca^{2+} channel (Rose et al., 1992). Thus, even in cardiac muscle, the DHPRs and the RyRs appear to be located in close proximity with each other, presumably within 20 nm (Sham et al., 1995*a*; Cannell et al., 1995). This unique spatial arrangement of both receptors possibly in combination with the recently described phenomenon of ryanodine receptor adaptation (Györke and Fill, 1993; Yasui et al., 1994; Valdivia et al., 1995) may be the primary reason for the "paradoxical" stable large amplification of CICR observed in cardiac myocytes, provided that there is no significant interaction among elementary Ca^{2+} release units (Stern, 1992; Cannell et al., 1995; Lopez-Lopez et al., 1995).

In the present study, we have co-expressed in chinese hamster ovary (CHO) cells the skeletal RyRs (Takeshima et al., 1989), α_2, β, and γ DHPR subunits and a chimeric DHPR α_1 subunit which possesses the regions critical for skeletal-type E-C coupling while conducting cardiac-like Ca^{2+} current (Tanabe et al., 1990). The purpose of the present study was to investigate possible interactions between these two channels in nonmuscle cells. The cotransfected CHO cells released Ca^{2+} through the RyRs following depolarization, but the Ca^{2+} release required entry of extracellular Ca^{2+}. Furthermore, the rate of increase in $[Ca^{2+}]_i$ due to Ca^{2+} release was much slower than that of cardiac myocytes, although the activation rate of Ca^{2+} current was similar. These results are compatible with the spatial arrangement of both receptors described for this preparation (Takekura et al., 1995*b*). Some aspects of this work appeared in an abstract form (Suda et al., 1996).

METHODS

Cell Preparation and Transfection

For details about construction of expression plasmids, transfection, RNA-, and immunoblotting analysis and other molecular biological methods, see Takekura et al. (1995*b*). Briefly, CHO cells were transfected with plasmids pRRS11 (for skeletal RyR) and pCAS8 (for chimeric DHPR α_1 subunit) in addition to pCAS7, pCAS14, and pCAS15 (for α_2, β, and γ subunits of the DHPR, respectively). G418-resistant clones were screened by RNA-blotting analysis (Takeshima et al., 1989) which gave positive results for all expected components. Expression of the RyRs and the chimeric DHPRs were confirmed by immunoblotting analysis (Takeshima et al., 1989) using monoclonal antibodies against the skeletal RyR and the cardiac DHPR, respectively. [^{3}H]Ryanodine binding assay and PN200-110 binding assay also confirmed expression of the RyRs and the chimeric DHPRs, respectively.

Cells were plated on coverslips and cultured at 37°C and 10% CO_2 in MEM-α (without nucleoside) medium (GIBCO BRL, Gaithersburg, MD) supplemented with FBS (10%), glutamine (2 mM), penicillin (0.06 mg/ml), streptomycin (0.11 mg/ml), and Na-pyruvate (1 mM).

Electrophysiological and Fluorescence Recordings

Combined patch-clamp and Fura-2 measurements were performed with a computer-controlled data acquisition system (EPC-9, HEKA, Lambrecht, Germany). The tight-seal whole-cell configuration was used to control membrane voltage and measure ionic current. Liquid junction potential correction (+8 mV) was made before seal formation when patch-pipette solution contained glutamate as the major anion. Capacitive currents were determined and compensated before each voltage pulse using the automatic capacitance compensation feature of the EPC-9. The holding potential was usually −70 mV. Currents were low-pass filtered (8-pole Bessel) at a corner frequency of 3.0 kHz and digitized at 100-μs intervals. For gating current experiments, the currents were filtered at 5 kHz and digitized at 40-μs intervals. To remove residual linear capacitive and leakage currents in the test

currents, 4 or 6 scaled, hyperpolarizing control voltage steps (each one-fourth or one-sixth the magnitude of the corresponding test step) were given before applying test pulses (P/−4 or P/−6). For presentation of figures, currents were digitally filtered at 3 kHz. Spatially averaged $[Ca^{2+}]_i$ was monitored with a photomultiplier based system where two fluorescence intensities were sampled at 2–10 Hz by a computer-driven charting program. Emission was measured at 500 nm, while excitation centered at 360 and 390 nm (in some experiments excitation was at 350 and 380 nm). An in situ calibration was made to estimate the absolute value of $[Ca^{2+}]_i$ as described previously (Suda and Penner, 1994). We used BAPTA [bis(2-aminophenoxy)ethane-N,N,N′,N′-tetraacetate] (Molecular Probes, Inc., Eugene, OR) for adjusting $[Ca^{2+}]_i$ in the calibration solutions, assuming a dissociation constant of 225 nM (Harrison and Bers, 1987). Usually, depolarizing pulses were started 200–250 s after obtaining the whole-cell configuration when fluorescence intensities approached steady levels. Experiments were performed at room temperature (22–25°C).

Solutions and Chemicals

Standard extracellular saline contained (in mM): TEA-Cl 150, $CaCl_2$ 3-5, $MgCl_2$ 1, glucose 11, Hepes 10, pH 7.2. Nominally Ca^{2+}-free saline was made by replacing Ca^{2+} with an equimolar concentration of Mg^{2+}. Gating currents were measured while applying nominally Ca^{2+}-free saline (plus appropriate amounts of $MgCl_2$ as suggested by Pizarro et al., 1989) or a standard saline to which 1–2 mM Cd^{2+} and 0.1 mM La^{3+} were added. For Ca^{2+} current measurements as illustrated in Fig. 1, external saline contained (in mM): NaCl 145, KCl 2.8, $CaCl_2$ 10, $MgCl_2$ 1, TEA-Cl 10, Hepes 10, glucose 11. Sylgard-coated patch-pipettes (Kimax) had resistances between 2–3 MΩ after filling with internal solution containing (in mM): Cs-glutamate 145, Fura-2 (potassium salt; Molecular Probes) 0.07–0.1, NaCl 8, Mg-ATP 6, Na_2-ATP 2, Hepes-CsOH 10, pH 7.2. The free magnesium concentration is calculated to be 0.35 mM, with an assumed affinity constant of 6.9×10^3 M^{-1} for Mg^{2+} binding to ATP. In some experiments, the following internal solution was used (in mM): Cs-glutamate 145, Fura-2 0.07–0.1, NaCl 8, Mg-ATP 7, Na_2-ATP 1, Hepes-CsOH 10, pH 7.2. The free magnesium concentration of this solution is calculated to be 0.6 mM. For Ca^{2+} current measurements as illustrated in Fig. 1, the pipette solution contained (in mM): *N*-methyl-D-glucamine145, NaCl 8, $MgCl_2$ 2, Cs-EGTA 20, Mg-ATP 4, GTP 0.3, Hepes 10, pH 7.2. Drug application was made by local ejection from wide-tipped pipettes. When tetracaine (100 μM, Sigma Chemical Co., St. Louis, MO) was used, the saline contained 7 mM Ca^{2+}. Usually, 10 mM caffeine (Sigma Chemical Co.) was applied in nominally Ca^{2+}-free saline. But in the experiments as illustrated in Fig. 5, caffeine (2 mM) was applied in 3 mM Ca^{2+} solution. All chemicals were of analytical grade.

Ca^{2+} Current Density in Cardiac Myocytes and Transformed CHO Cells

The apparent Ca^{2+} current density of the cotransfected CHO cells, that exhibited CICR, varied from 34 to 160 pA/pF and was on average 74 ± 44 pA/pF (mean ± SEM) at +20 mV ($n = 10$). These values were measured 250–400 s after obtaining the whole-cell configuration with 0.1 mM Fura-2 as the only exogenous Ca^{2+} chelator. In cardiac myocytes, peak inward Ca^{2+} current is at most 2 nA for both rat and guinea-pig ventricular cells and the cell surface area (including T-tubules) is estimated to be larger than $6–7 \times 10^{-5}$ cm^2 (e.g., Callewaert et al., 1988; Cannell et al., 1995) Thus, assuming a specific membrane capacitance of 1 μF/cm^2, the current density would be at most 30 pA/pF. Actual reported values in the literatures are much smaller (<10 pA/pF) than this (e.g., Sham et al., 1995*b*). Therefore, it is clear that the apparent current densities of the cotransfected CHO cells that exhibited CICR were much larger than the upper limit of those of cardiac myocytes. With "low" Ca^{2+} current densities (<20 pA/pF), CICR was not detected in this preparation.

RESULTS

Ca^{2+} Currents of Transformed CHO Cells Are Similar to Ca^{2+} Currents in Cardiac Cells

Because the putative transmembrane regions of the chimeric DHPR expressed in the transfected CHO cells are of cardiac origin, the characteristics of the Ca^{2+} current are expected to be similar to those of cardiac myocytes (Tanabe et al., 1990). In Fig. 1 *A*, the cell was bathed in a saline containing 5 mM extracellular Ca^{2+} concentration ($[Ca^{2+}]_o$). Depolarizing pulses of 150-ms duration were applied from a holding potential of −70 mV to various test potentials, in 20-mV increments. Inward currents were evoked by depolarizations between −30 mV and +80 mV, while more positive voltages evoked small outward currents. Peak inward currents were measured around +10 mV (Fig. 1 *B*). A fit to the mean current-voltage curve yielded values for $V_{1/2}$ of +4 mV and a slope factor of +11 mV. The activation time constant of the current was on the order of 1–3 ms (Fig. 1 *C*) and similar to L-type Ca^{2+} current present in native cardiac myocytes (data not shown). Inward currents were strongly reduced in nominally Ca^{2+}-free saline and were completely blocked by low concentrations (0.5–1 μM) of the dihydropyridines, PN200-110 ($n = 4$; see Fig. 1 *D*), nifedipine ($n = 3$), and nimodipine ($n = 2$), or 1–2 mM Cd^{2+} ($n = 10$). Peak inward currents were significantly increased and the decay of the tail current was slowed by 1 μM Bay-K 8644 ($n = 2$). These results, taken together, confirm that the current reflected Ca^{2+} flux through the dihydropyridine-sensitive Ca^{2+} channels. No such currents were detected in nontransfected CHO cells ($n = 10$; data not shown).

Cotransfected CHO Cells Exhibit Different Patterns of Ca^{2+} Transients

The transformed cells used in the present study also expressed type-1 RyRs, which are intracellular Ca^{2+} release channels not normally found in CHO cells (Takekura et al., 1995*b*). We used relatively low concentrations of Mg^{2+} (0.35–0.6 mM) and a high concentration of total ATP (8 mM) in the internal solutions to provide favorable conditions for activation of RyRs (Meissner, 1994), with 0.1 mM Fura-2 being the only exogenous Ca^{2+} chelator. Under these conditions, basal $[Ca^{2+}]_i$ was usually between 50 and 300 nM, except when spontaneous $[Ca^{2+}]_i$ oscillation occurred. 5 mM $[Ca^{2+}]_o$ was the upper limit to maintain the basal $[Ca^{2+}]_i$ below 300 nM.

Application of 5–10 mM caffeine confirmed that large CaTs could be induced in the absence of $[Ca^{2+}]_o$ (e.g., Fig. 4 *C*; $n > 24$). Furthermore, ~10% of the tested cells exhibited spontaneous $[Ca^{2+}]_i$ oscillations in 3–5 mM $[Ca^{2+}]_o$, even though the membrane potential was clamped at −70 mV ($n = 11$; Fig. 2 *A*). In these cells, basal $[Ca^{2+}]_i$ was usually higher than 0.4 μM and depolarizing voltage pulses, which normally would produce a CaT (see below), occasionally failed to induce a CaT, possibly due to inactivation of Ca^{2+} currents at high concentrations of global $[Ca^{2+}]_i$. When removing $[Ca^{2+}]_o$, basal $[Ca^{2+}]_i$ decreased and the oscillation frequency was reduced (Fig. 2 *A*; $n = 3$). Addition of 100 μM tetracaine not only decreased the basal $[Ca^{2+}]_i$ but terminated the oscillations completely ($n = 5$; data not shown), suggesting that these oscillatory events occurred through pulsatile release of Ca^{2+} through RyRs. This, together with the Ca^{2+} current data presented above, establishes that the DHPRs and the RyRs form functional channels in the surface membrane and the membranes of internal stores, respectively. This stands in good agreement with immunoblotting analysis (Takekura et al., 1995*b*).

The next question we asked was whether these two channels located in distinct membranes are able to communicate with each other. Fig. 2, *B–D* show examples of three representative CaTs evoked by depolarizing pulses to +20 mV (250 ms) at 60-s intervals in different cells. In all cases, a transient increase in $[Ca^{2+}]_i$ occurred immediately after depolarization. Such depolarization-induced CaTs were only observed when the cells were bathed in Ca^{2+}-containing saline (usually 5 mM $[Ca^{2+}]_o$). In some cells, the CaT returned to baseline with a monoexponential time course, whereas in others the rapid $[Ca^{2+}]_i$ spike was followed by a secondary, slower rise in $[Ca^{2+}]_i$ (Fig. 2, *C* and *D*).

To assess the CaTs in a more quantitative manner, we analyzed them as illustrated in Fig. 3. The criterion used to distinguish the two phases is based on the break point where the time derivative of the Ca^{2+} signal decreases (following the rapid rise in the Ca^{2+} signal). Thus, the fast initial component appears in <0.75 s after the onset of depolarization and reaches 95% of its peak value within 0.6 s. Subsequently, $[Ca^{2+}]_i$ continues to rise in cells that exhibit a second component, but at significantly decreased rates. Our results suggest that the first component primarily reflects an increase in $[Ca^{2+}]_i$ due to Ca^{2+} current, whereas the second component reflects an increase in $[Ca^{2+}]_i$ due to Ca^{2+} release through the RyRs (Figs. 5 and 6). Throughout this article, we will refer to the ratio of the magnitude (i.e., the difference between peak and basal $[Ca^{2+}]_i$) of the secondary increase in $[Ca^{2+}]_i$ to that of the initial peak of the Ca^{2+} transient elicited by depolarization as the CaT_2/CaT_1 Ratio ("CaTR").

Based on the analysis of 98 cells (excluding those with $[Ca^{2+}]_i$ oscillations), we estimated that ~60% of the tested cells ($n = 60$) exhibited a rapid increase in

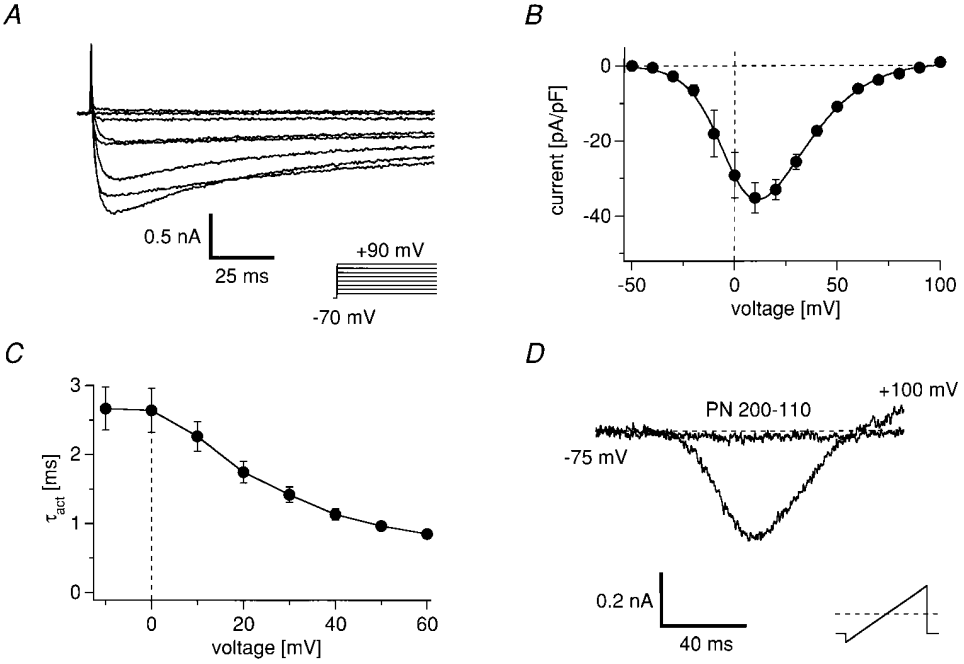

FIGURE 1. Ca^{2+} currents expressed in the cotransfected CHO cells. (*A*) Ca^{2+} currents evoked by different depolarizing pulses. The currents were recorded in 5 mM $[Ca^{2+}]_o$. Upper traces represent membrane voltage and lower traces Ca^{2+} current. Depolarizing pulses of 150-ms duration were applied from a holding potential of −70 mV to various test potentials, ranging from −50 to +90 mV, in 20-mV increments. (*B*) Currents versus voltage relationships. The maximum peak inward current was between +20 and +30 mV. Filled circles indicate mean values. Error bars indicate SEM ($n = 7$). (*C*) Activation time constant (τ_{act}) of Ca^{2+} current. Current traces during activation were fitted by a single exponential function and the time constants plotted versus voltages ($n = 7$). (*D*) Block of Ca^{2+} current by a DHP antagonist. 0.5 μM PN200-110 completely blocked the current evoked by a ramp pulse (−100 to +100 mV, 50 ms) ($n = 5$).

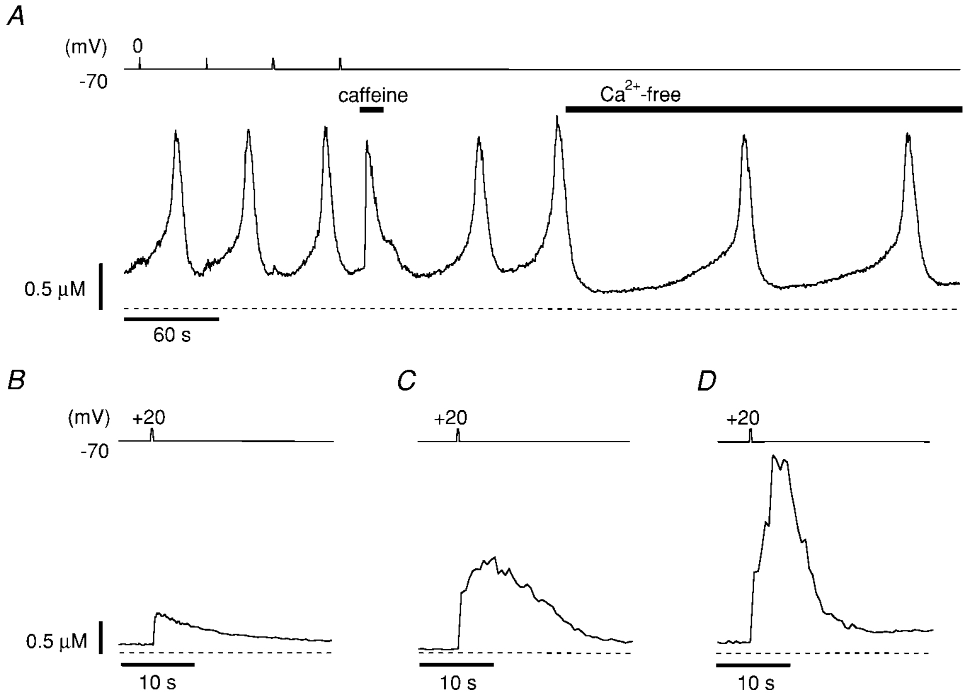

FIGURE 2. Different patterns of Ca^{2+} transients. Upper trace indicates membrane voltage and lower trace $[Ca^{2+}]_i$. Data were taken from different cells. (*A*) $[Ca^{2+}]_i$ oscillation. The cell was bathed in 3 mM $[Ca^{2+}]_o$ and the holding potential was −70 mV. The patch-pipette contained 0.35 mM Mg^{2+}. The Ca^{2+} transient induced by 10 mM caffeine had almost the same amplitude as the peaks of the oscillation. Note that depolarization failed to induce a Ca^{2+} transient. In nominally Ca^{2+}-free saline, both basal $[Ca^{2+}]_o$ and the oscillation frequency decreased but the threshold for regenerative Ca^{2+} release was unaffected. (*B*) Depolarization-induced Ca^{2+} transient exhibiting a single exponential decay. After fluorescence signals approached steady levels, depolarizing pulses to +20 mV (250 ms) were applied every 60 s in 5 mM $[Ca^{2+}]_o$. C_m = 18.5 pF. (*C*) Depolarization-induced Ca^{2+} transient with two kinetic components: a transient increase in $[Ca^{2+}]_i$ (the first component) followed by a sustained secondary increase in $[Ca^{2+}]_i$ (the secondary component). The same protocol as used in *B*. The ratio of the amplitude of the secondary component to that of the first component was small in this cell (CaTR < 1.7). C_m = 50 pF. (*D*) Depolarization-induced Ca^{2+} transient exhibiting a relatively large secondary component (CaTR > 2.5). The same stimulus protocol as used in *B*. C_m = 26 pF.

$[Ca^{2+}]_i$ (the first component in Fig. 3) followed by single-exponential decay to baseline (Fig. 2 *B*), whereas the others showed a sustained secondary increase in $[Ca^{2+}]_i$ (the second component in Fig. 3) lasting for 5–10 s (n = 38). In the latter case, the ratio of the amplitude of the peak of the second component to that of the first component ("CaTR") varied from cell to cell. While some cells exhibited a rather small ratio (e.g., Fig. 2 *C*: CaTR = 1.64), others had large ratios (e.g., CaTR = 2.69; Fig. 2 *D*). The size of the second component also varied from cell to cell, ranging between 0.7 and 3.4 µM. In general, the second component was gradually reduced and ultimately disappeared at later times during a lengthy experiment. However, as long as a relatively large ratio appeared at the first pulse (e.g., CaTR > 2.0), the second component was invariably present at least for the first 6–7 pulses (n = 12).

Recently, Takeshima et al. (1994) and Nakai et al. (1996) directly demonstrated that the skeletal RyR iso-

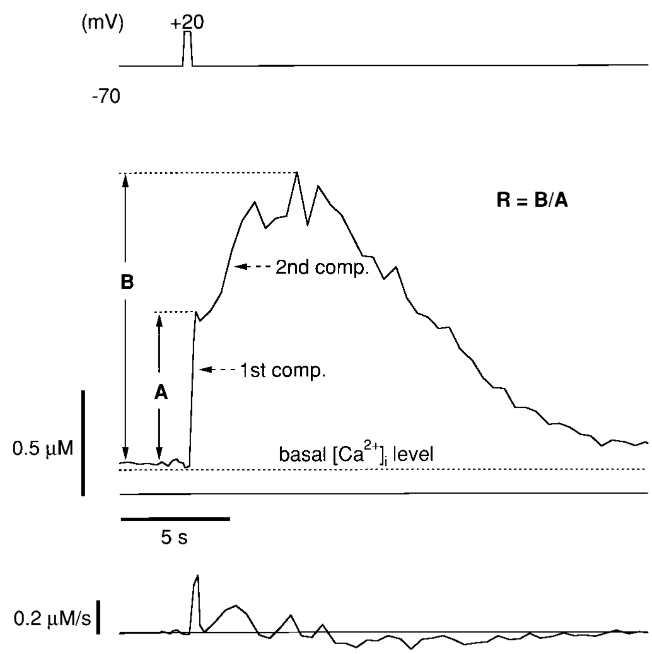

FIGURE 3. Definition of calcium transient ratio ("CaTR"). The magnitude of the secondary Ca^{2+}-transient component (*B*; this component reflects Ca^{2+} release through the RyRs) to that of the first component (*A*; this component primarily reflects Ca^{2+} influx through Ca^{2+} channels) is referred to as Calcium Transient Ratio (CaTR = B/A). In this example, CaTR = 1.89 (the cell was depolarized to +20 mV for 250 ms in 5 mM $[Ca^{2+}]_o$.) The first component peaks at 0.5 s after the onset of depolarization and then the second component develops slowly, reaching its peak at 5.3 s after depolarization. Note that the time derivative of $[Ca^{2+}]_i$ ($d[Ca^{2+}]_i/dt$) decreases after the peak of the first component. When the initial peak was not clearly discernible, we analyzed the point where $d[Ca^{2+}]_i/dt$ started to decrease. The time to peak of the first component was invariably < 0.75 s (n = 40).

form functions as the physiological voltage-gated Ca^{2+} release channel. Because the chimeric DHPR expressed in the transformed CHO cells possesses the regions critical for interacting with the release channels (Tanabe et al., 1990), the following possibilities may explain the two components of the CaT, provided that the second component does not reflect a saturation of Ca^{2+}-buffering capacity: (*1*) voltage-gated Ca^{2+} release from internal stores, (*2*) Ca^{2+} influx through Ca^{2+} channels, (*3*) CICR from internal stores, and (*4*) a combination of two or all of these factors.

Cotransfected CHO Cells Lack Voltage-gated Ca^{2+} Release

First, we examined whether voltage-gated Ca^{2+} release, an essential property of skeletal-type E-C coupling, is reconstituted in cotransfected CHO cells. As illustrated in Fig. 4 *A*, depolarizing pulses to +20 mV (250 ms) in the presence of 5 mM $[Ca^{2+}]_o$ evoked a large CaT with two kinetic components. In nominally Ca^{2+}-free saline, however, the CaT evoked by the same pulse was markedly reduced (n = 13; Fig. 4 *B*). The small CaT might reflect a residual Ca^{2+} current since we had not added EGTA to the external solution. Furthermore, stronger depolarizations (e.g., +90 mV), where the net Ca^{2+} influx probably was zero, did not evoke any detectable rise in $[Ca^{2+}]_i$ (Fig. 4 *B*). The reduction or abolition of a CaT in nominally Ca^{2+}-free saline was not attributable to depletion of stored Ca^{2+}, as 10 mM caffeine still induced a large rapid increase in $[Ca^{2+}]_i$ under the same conditions (Fig. 4 *C*). Depolarization also failed to induce a CaT in nominally Ca^{2+}-free saline at quite negative holding potentials (−100 to −120 mV). Thus, absence of voltage-gated Ca^{2+} release in nominally Ca^{2+}-free saline is unlikely to be due to an effect of Ca^{2+} deprivation on the voltage sensors (Brum et al., 1988*a*, *b*; Pizarro et al., 1989).

As illustrated in Fig. 4 *E*, the cells exhibited large gating currents which appeared at −30 mV and gradually increased, reaching 66.8 ± 25.6 nC/μF (n = 6) at +60 or +70 mV. These values are larger than Q_{max} values obtained from native mammalian skeletal muscle (15.8 − 46.2 nC/μF; Rios and Pizarro, 1991). Because charge movement does not significantly differ among skeletal, cardiac, and chimeric DHPRs when expressed in dysgenic myotubes (Adams et al., 1990), the expression level of the DHPRs in the transfected CHO cells is at least as high as functional voltage sensors in native skeletal muscles, assuming the same gating charge to be re-

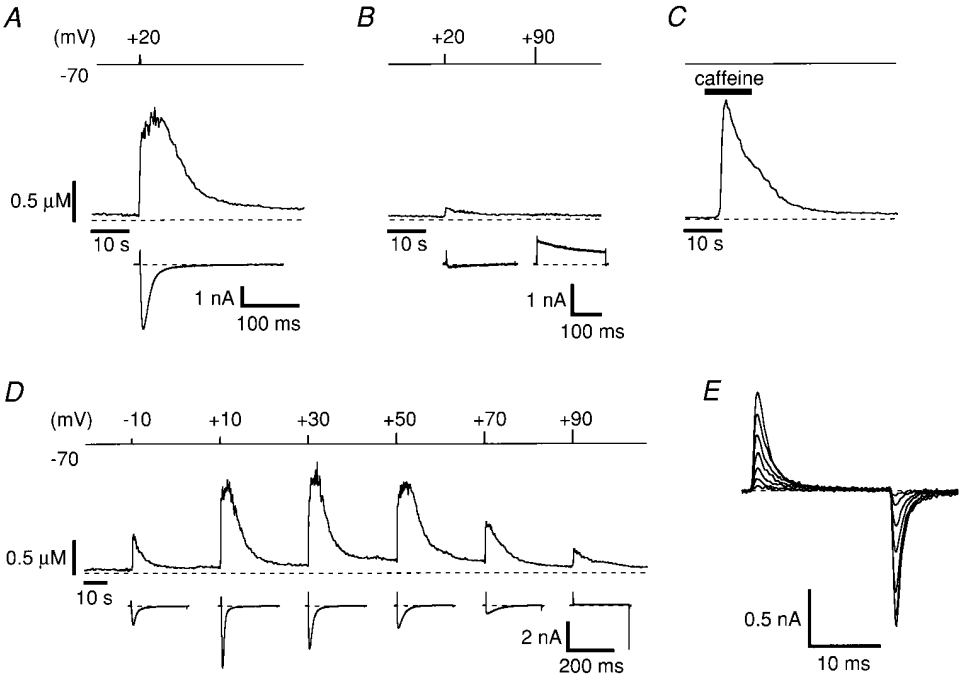

FIGURE 4. No indication of skeletal-type E-C coupling. *A–D* are taken from the same cell. (*A*) Control experiment. Upper traces represent membrane voltage, middle traces $[Ca^{2+}]_i$, and the bottom traces Ca^{2+} current. In the presence of $[Ca^{2+}]_o$ (5 mM), depolarization to +20 mV (250 ms) evoked a large Ca^{2+} transient exhibiting a CICR component. Total integrated charge carried by the inward current was 81.09 pC. (*B*) In nominally Ca^{2+}-free saline, the Ca^{2+} transient elicited by a +20 mV dpolarization was reduced due to a reduction in the Ca^{2+} current. Total integrated charge carried by the inward current was 12.6 pC. Depolarization to +90 mV (250 ms) no longer produced any change in $[Ca^{2+}]_i$. (*C*) Caffeine-induced Ca^{2+} transient in nominally Ca^{2+}-free saline. After applying several depolarizing pulses in nominally Ca^{2+}-free saline for 120 s, 10 mM caffeine was applied during the time indicated. (*D*) Ca^{2+} transients versus voltage relationships. The cell was bathed in 3 mM $[Ca^{2+}]_o$ and was dialyzed with 0.35 mM $[Mg^{2+}]_i$. Depolarizing pulses of 250 ms duration were applied repetitively every 40 s ranging from −10 mV to +90 mV, in 20-mV increments. The corresponding current traces are shown at the bottom. Total integrated charge carried by the inward currents were 46 pC (−10 mV), 78.5 pC (+10 mV), 77.9 pC (+30 mV), 58.1 pC (+50 mV), and 38.3 pC (+70 mV). C = 22 pF. (*E*) Gating currents associated with chimeric DHPR-Ca^{2+} channels. Gating currents were measured in 5 mM $[Ca^{2+}]_o$ while blocking Ca^{2+} current by both 1 mM Cd^{2+} and 0.1 mM La^{3+}. The holding potential was −80 mV. Depolarizing pulses of 10-ms duration were applied repetitively at 2-s intervals, ranging from −60 mV to +70 mV, in 20-mV increments. The control currents were elicited from −120 mV. The amount of charge moved at +60 and +70 mV were, respectively, 1.1 pC and 1.2 pC for both on and off gating. C_m = 23.9 pF.

quired to activate either species of channel. No such gating currents were detected in nontransfected CHO cells (data not shown).

Clearly, in contrast to skeletal muscle, CaTs did not exhibit a sigmoidal voltage dependence (Fig. 4 *D*; $n = 7$) and CaTs were smaller at stronger depolarization ($n = 17$), presumably due to a smaller amount of Ca^{2+} influx. This suggests that, unlike in skeletal muscle, DHPRs and RyRs do not interact directly in cotransfected CHO cells (but see Discussion). Thus, CaTs elicited by depolarization in the presence of $[Ca^{2+}]_o$ probably reflected Ca^{2+} influx alone or a combination of both Ca^{2+} influx and CICR.

The Second Component of Ca^{2+} Transient Is Due to Release from Internal Stores

To see whether CICR is involved in producing CaTs, we tested the effect of tetracaine, a CICR inhibitor, on the second component of the CaT. Since tetracaine caused a slight inhibition of Ca^{2+} currents, we increased $[Ca^{2+}]_o$ in the tetracaine-containing solution to 7 mM to compensate for the effect of tetracaine on DHPRs. This produced almost the same amount of total Ca^{2+} influx as compared to control (e.g., compare the 2nd and 3rd pulses in Fig. 5 *B*).

Fig. 5 *A* illustrates a control experiment, in which the ratio of the amplitude of the second component to that of the first component was relatively large (CaTR > 2.5). It is seen that repetitive stimulation evoked similar-sized Ca^{2+} currents and CaTs under control conditions (the first four CaTs of the cell are shown). However, application of 100 μM tetracaine strongly reduced the second component (Fig. 5 *B*). Similar results were obtained in seven other cells, two of which exhibited complete abolition of the second component.

Conversely, cells that exhibited only the first component of CaT revealed a large second component in the presence of a subthreshold concentration of caffeine (2 mM), despite a smaller amount of Ca^{2+} influx ($n = 6$; Fig. 5 *C*).

No Indication of CICR in CHO Cells Expressing Only DHPR Subunits

We conducted control experiments using CHO cells expressing only DHPRs (−RyR) to confirm that solely CHO cells co-expressing DHPRs and RyRs (+RyR) are able to show Ca^{2+} release. In Fig. 6 *A*, CaTs from single-transfected (−RyR) and cotransfected (+RyR) CHO cells are superimposed in order to compare the time course of CaTs (induced by 250 ms depolarization to +20 mV in 5 mM $[Ca^{2+}]_o$). Depolarization-evoked CaTs in single-transfected CHO cells decayed monoexponentially after the first rapid peak (0.6 s after depolarization in this case) and invariably failed to exhibit any secondary increase in $[Ca^{2+}]_i$. The shape of the CaTs in the single-transfected cells (−RyR) was similar to those CaTs in (+RyR) cells that did not show a secondary phase.

Fig. 6 *B* plots the maximum depolarization-induced increase of $[Ca^{2+}]_i$ against the normalized Ca^{2+} current integral of both (−RyR) and (+RyR) cells without a plateau phase. It is seen that the two regression lines fit-

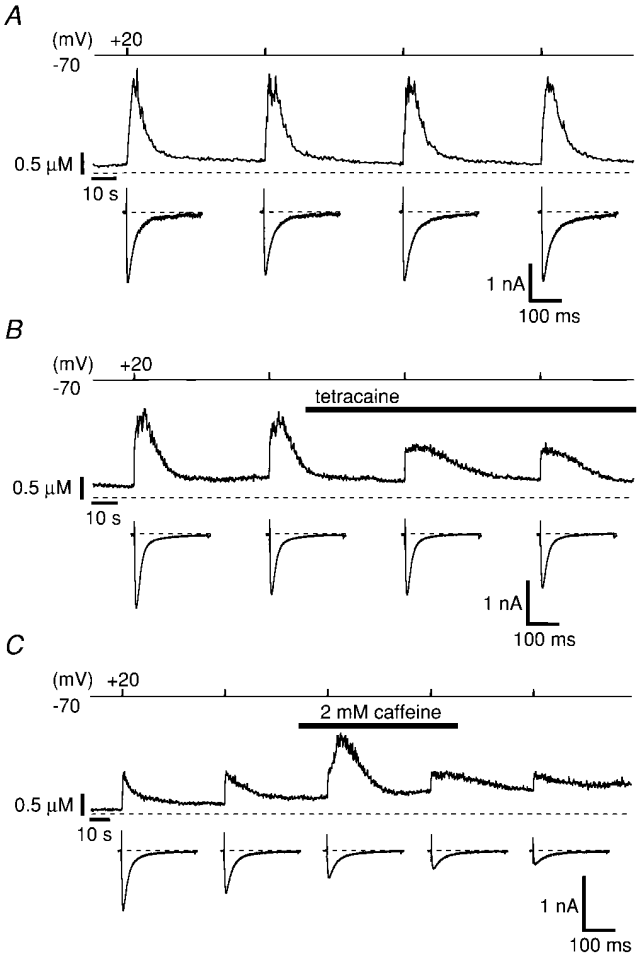

FIGURE 5. The second component of Ca^{2+} transient is due to Ca^{2+} release through the ryanodine receptor-Ca^{2+} release channels. Data are taken from different cells. (*A*) Control experiment. Upper traces represent membrane voltage, middle traces $[Ca^{2+}]_i$, and bottom traces Ca^{2+} current. Depolarizing pulses to +20 mV (250 ms) were applied repetitively at 60-s intervals in 5 mM $[Ca^{2+}]_o$. The pulses were started 300 s after obtaining the whole-cell configuration. The first four Ca^{2+} transients exhibiting a large second component are shown. The cell was dialyzed with 0.35 mM $[Mg^{2+}]_i$. $C = 44$ pF. (*B*) Tetracaine reduced the second component. The same protocol as used in *A* except that 100 μM tetracaine was applied following the second pulse. Total integrated charge carried by the inward currents during the second and third pulses were 47.0 pC and 42.3 pC, respectively. (*C*) Subthreshold level of caffeine induced the second component. The same protocol as used in *A* except that 2 mM caffeine was applied in 3 mM $[Ca^{2+}]_o$ during the time indicated. The Ca^{2+} transient evoked by the fourth pulse did not exhibit the second component, presumably due to either desensitization or a reduction in Ca^{2+} influx.

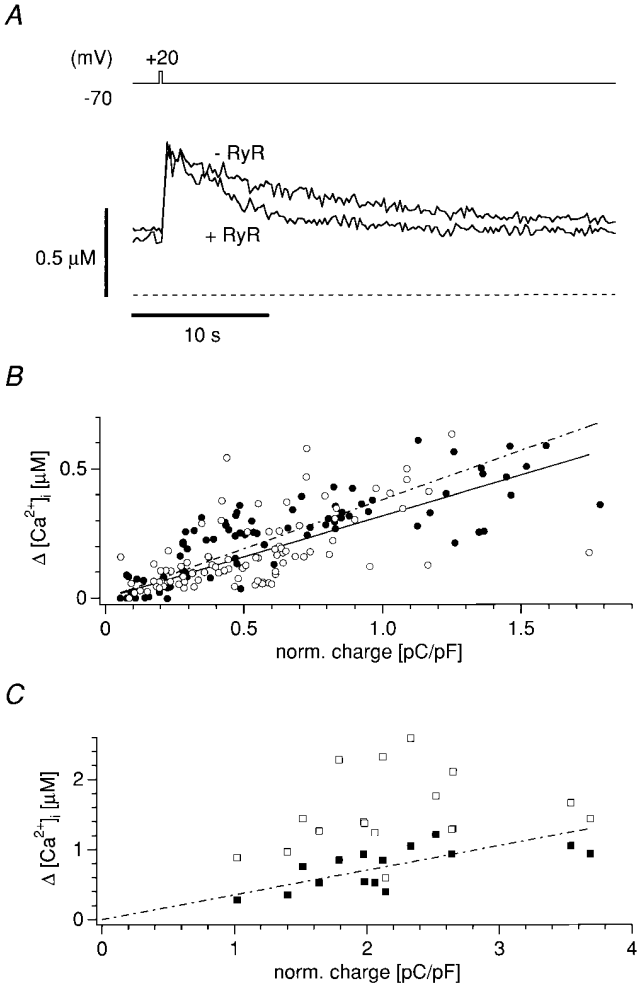

FIGURE 6. Depolarization-induced $[Ca^{2+}]_i$ changes in DHPR-transfected CHO cells with or without cotransfection of RyR. (*A*) Superimposed Ca^{2+} transients evoked by a 250-ms depolarization to +20 mV in 5 mM $[Ca^{2+}]_o$. DHPR-transfected CHO cells without RyR (−RyR) are represented by the thick line and with (+RyR) are superimposed. Cells of similar size were chosen (36 ± 2 pF for −RyR, $n = 3$; 30 ± 5 pF for +RyR, $n = 3$.). Time to peak was 0.6 s in both traces. (*B*) Depolarization-induced changes in $[Ca^{2+}]_i$ in DHPR-expressing CHO cells without (*open circles*; $n = 31$) or with (*filled circles*; $n = 24$) RyR coexpression as a function of total charge carried by Ca^{2+} current normalized to linear capacitance of the cells. Ca^{2+} transients were evoked by a 250-ms depolarization to +20 mV in 5 mM $[Ca^{2+}]_o$. 1–5 data points could be obtained per cell. To evaluate the change in $[Ca^{2+}]_i$ induced by each depolarization, the initial peak value of the Ca^{2+} transient and peak of the second component was measured as the difference from the basal $[Ca^{2+}]_i$ preceding the depolarization. The last three data points before the depolarization were averaged to yield basal $[Ca^{2+}]_i$ and the CaT amplitude was determined from the peak $[Ca^{2+}]_i$. The two data sets were fitted with a linear regression line. (*C*) Depolarization-induced changes in $[Ca^{2+}]_i$ in cotransfected CHO cells. Ca^{2+} transients were evoked by a 250-ms depolarization to +20 mV in 5 mM $[Ca^{2+}]_o$ except in one experiment where the pulse duration was 200 ms. Peaks of the first component (■) fall on the regression line which is the average of the two regression lines illustrated in *B*, whereas the peaks of the secondary component (□) deviate from it.

ted to the respective data sets do not differ significantly, supporting the idea that monoexponentially decaying CaTs reflect Ca^{2+} influx through Ca^{2+} channels rather than Ca^{2+} release. The analysis of cotransfected cells producing a plateau phase is shown in Fig. 6 *C*. Here, the peaks of the first component as well as the second component are plotted against the normalized charge (current integral) of the respective Ca^{2+} currents. It is seen that while the maximal amplitudes of the first component (■) are well described by the regression line fitted to (+RyR) cells, the peaks of the second component (□) deviate significantly. This further supports the notion that the first component appears to primarily reflect Ca^{2+} influx through Ca^{2+} channels and that CICR is associated with expression of RyRs.

Separation of Two Kinetic Components in All-or-None Type Ca^{2+} Transient

To further establish that the second component is indeed caused by Ca^{2+} release from internal stores and not a consequence of saturation of the Ca^{2+}-buffering capacity of the cell, we reduced CICR activity by increasing $[Mg^{2+}]_i$ to 0.6 mM and reducing $[Ca^{2+}]_o$ to 2 mM. These conditions were deemed sufficient to inhibit CICR, because the skeletal muscle RyR isoform is less sensitive to Ca^{2+} than the cardiac isoform and because the distance between the DHPRs and the RyRs appears to be much larger than in cardiac myocytes, as will be discussed later. CaTs exhibiting a secondary component were rare under these conditions. However, four cells did show CaTs with a plateau phase that seemed to occur almost in an all-or-none manner, since the same pulse (+20 mV, 200 ms) produced completely different patterns of CaTs within one cell.

The data in Fig. 7 *A* provide an example in which the first and the second components were clearly separated. It should be pointed out that the secondary component developed after the first component already started to decay, which indicates that the second component does not reflect a saturation of Ca^{2+}-buffering capacity. Similarly dissociated CaTs were observed in five other cells, regardless of the individual CaTR.

The possibility remains that not only the amount of Ca^{2+} entry but also the filling state of internal Ca^{2+} stores may be an important determinant of the amount of Ca^{2+} release in this preparation. We therefore checked whether the pulse intervals of 40–60 s used in this study were appropriate to allow refilling of caffeine-sensitive pools. To this end we applied 10 mM caffeine during an interpulse interval to see whether such a caffeine-induced CaT would alter the shape of a subsequent depolarization-induced CaT (Fig. 7 *B*). However, the size of the CICR component evoked by a depolarization to +20 mV was not significantly affected by a preceding caffeine-induced Ca^{2+} release ($n = 5$).

This suggests that a large fraction of the Ca^{2+} ions released by caffeine could be taken up again by the stores within 30 s and contribute to the next release phase.

Global Increase in $[Ca^{2+}]_i$ Rather Than Local Increase in $[Ca^{2+}]_i$ Determines the Amount of Ca^{2+} Release

Finally, we posed the question whether the amount of Ca^{2+} release is determined by either a global increase in $[Ca^{2+}]_i$ or rather a local one. If the global increase in $[Ca^{2+}]_i$ is the important determinant of triggering Ca^{2+} release, then the integral of the Ca^{2+} current rather than the peak amplitude will determine the amount of Ca^{2+} release. To test this, we conducted experiments where the cell was depolarized at 40-s intervals to the same potential (+20 mV) but with increasing pulse duration (Fig. 8). It is seen that the CaTs elicited by depolarizing pulses of longer than 100 ms clearly exhibited two kinetic components in which the second component grew as the depolarizing pulse duration was increased (Fig. 8 *A*, 175-ms and 250-ms pulse durations). Similar results were obtained when reversing the stimulus protocol by decreasing the pulse duration (Fig. 8 *B*). According to Stern's theory (1992) a low-gain system would require only very little additional Ca^{2+} influx in order to produce such a graded response in CICR. It is noteworthy that in this preparation DHPRs inactivated and thus only a small change in total Ca^{2+} influx was able to produce a relatively large change in $[Ca^{2+}]_i$. Therefore, one might argue that the total amount of Ca^{2+} influx rather than the peak current amplitude appeared to determine the amount of Ca^{2+} release in these cells ($n = 9$).

DISCUSSION

CICR Is Reconstituted in the Cotransfected CHO Cells

The present study demonstrates that CHO cells, when co-expressed with the skeletal muscle RyR isoform and a chimeric DHPR, express both proteins as functional Ca^{2+} release channels and voltage-gated Ca^{2+} channels, respectively. Previous studies have established that type-1 RyR is responsible for voltage-gated Ca^{2+} release (Takeshima et al., 1994; Nakai et al., 1996) and that the chimeric DHPR expressed in CHO cells can in principle function as the voltage sensor of E-C coupling in dysgenic mouse myotubes (Adams et al., 1990). Although both channel proteins are expressed in high

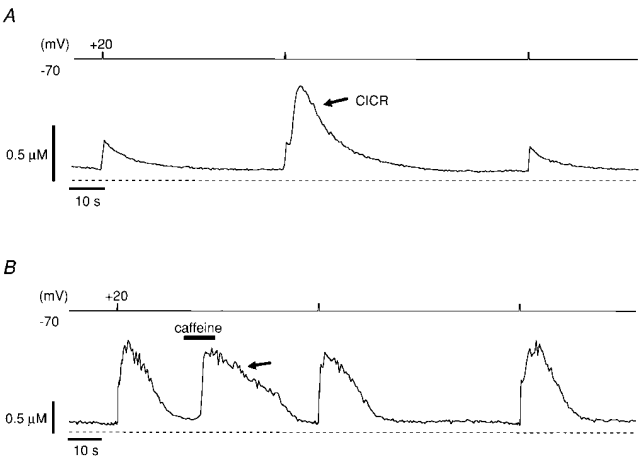

FIGURE 7. Separation of the two components of Ca^{2+} transients by threshold activation. (*A*) Upper trace represents membrane voltage and lower trace $[Ca^{2+}]_i$. The cell was bathed in 2 mM $[Ca^{2+}]_o$ and was dialyzed with 0.6 mM $[Mg^{2+}]_i$. Depolarizing pulses to +20 mV (200 ms) were applied approximately at 60-s intervals. The same pulse produced completely different shapes of Ca^{2+} transients. The peak of the first component elicited by the second pulse was smaller than that by the first pulse. Note the second component developed after a partial decay of the first component. C_m = 35.4 pF. (*B*) Replenishment of caffeine-sensitive Ca^{2+} pools. Ca^{2+} release induced by 10 mM caffeine had little effect on the second component of a subsequent Ca^{2+} transient induced by depolarization. The cell was bathed in 5 mM $[Ca^{2+}]_o$ and was dialyzed with 0.35 mM $[Mg^{2+}]_i$. Depolarizing pulses to +20 mV (250 ms) were applied approximately at 60-s intervals. 10 mM caffeine was applied between the second and third pulses, as indicated. C_m = 29 pF.

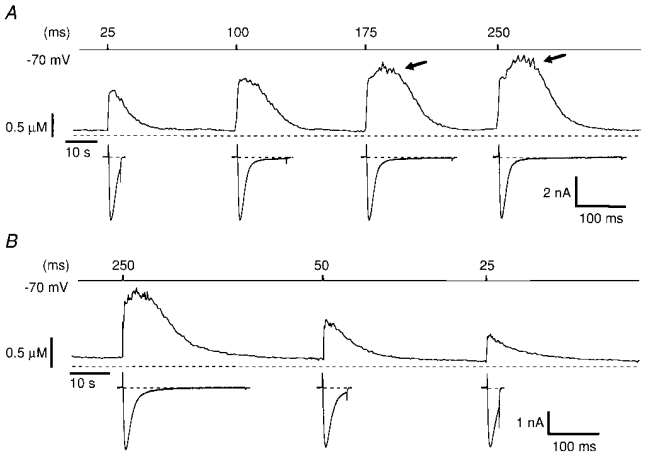

FIGURE 8. Effect of depolarizing pulse duration on the second component of the Ca^{2+} transient. Data were taken from different cells. (*A*) Effect of depolarizing pulse duration on CICR with small CaTR. Longer depolarizations produced larger second components. The upper trace shows membrane voltage, the middle trace $[Ca^{2+}]_i$, and the bottom trace Ca^{2+} current. The cell was bathed in 5 mM $[Ca^{2+}]_o$ and was dialyzed with 0.35 mM $[Mg^{2+}]_i$. Depolarizing pulses (+20 mV) of increasing duration were applied repetitively every 40 s after obtaining the whole-cell configuration for 240 s. Total integrated charge carried by the inward currents were 62.9 pC (25 ms), 81.5 pC (100 ms), 87.8 pC (175 ms), and 88.1 pC (250 ms). C_m = 33 pF. (*B*) Decreasing depolarizing pulse duration resulted in a reduction in the second component. The cell was bathed in 3 mM $[Ca^{2+}]_o$ and was dialyzed with 0.35 mM $[Mg^{2+}]_i$. Depolarizing pulses were applied repetitively at 40-s intervals over 710 s after obtaining the whole-cell configuration. Total integrated charge carried by the inward currents were 68.3 pC (250 ms), 55.8 pC (50 ms), and 44.9 pC (25 ms). C_m = 22 pF.

levels in CHO cells, there is no apparent reconstitution of voltage-gated Ca^{2+} release. However, we have obtained clear evidence for cross-talk between DHPRs and RyRs in the form of CICR.

The cotransfected CHO cells apparently exhibit two different patterns of CaTs. One pattern is similar to the CaT of control cells (expressing only with the DHPR), where a transient increase in $[Ca^{2+}]_i$ is followed by an exponential decay. The other pattern exhibits two kinetic components: a transient increase in $[Ca^{2+}]_i$ that is followed by a sustained secondary increase in $[Ca^{2+}]_i$ lasting 5–10 s. Because the peak of the second component is reduced by addition of tetracaine and is enhanced by subthreshold concentrations of caffeine, this component appears to reflect Ca^{2+} release from internal stores. Consistent with this, the second component is not observed in single-transfected CHO cells. Further confirmation comes from the fact that, under certain conditions, the same pulse produces completely different patterns of CaTs: either the first component or a combination of both the first and second components.

When the calcium-transient ratio (CaTR) is relatively large (e.g., $R > 3.0$), the Ca^{2+} release occurrs in an all-or-none rather than graded manner, and occasionally the second (CICR) component develops after a partial decay of the first component (Fig. 7). It is likely that once a fraction of the RyRs starts to release Ca^{2+} following a global increase in $[Ca^{2+}]_i$, the released Ca^{2+} ions in turn trigger neighboring RyRs, resulting in a further increase in $[Ca^{2+}]_i$. It is also possible that development of the second component after a partial decay of the first component reflects a transient inhibition of Ca^{2+} release by excessive Ca^{2+} influx, which resumes after dissipation of $[Ca^{2+}]_i$. On the other hand, when the CaTR is small (e.g., $R < 1.5$), the Ca^{2+} release occurs in a more graded manner (e.g., Fig. 8), which might be due to the much smaller overall gain of CICR in the transfected cells as compared to cardiac myocytes (Stern, 1992). However, the present results do not rule out other explanations for graded CICR such as adaptation (Györke and Fill, 1993; Yasui et al., 1994; Valdivia et al., 1995) or even as yet unknown mechanisms. In any case, it seems safe to assume that the second component reflects a regenerative Ca^{2+} release process and not a saturation of Ca^{2+}-buffering capacity.

It seems unlikely that the second component is due to Ca^{2+} release through the $InsP_3$ receptors, which are also present in these cells, because the amplitude of the $InsP_3$-induced CaT is much smaller than that of the caffeine-induced CaT, as previously reported (Penner et al., 1989). That the second component appears in the presence of a subthreshold concentration of caffeine (Fig. 5 *C*), an inhibitor of $InsP_3$-induced Ca^{2+} release, also argues against a major role for $InsP_3$-induced Ca^{2+} release. To test this point more directly, we dialyzed cells with 0.5 mg/ml heparin, a blocker of $InsP_3$ receptors. Under these conditions, the second component could be observed in 4 out of 4 cells and the largest CaTR observed was 2.5 (data not shown).

CICR of the Cotransfected CHO Cells Differs from That of Cardiac Myocytes

While the present study suggests that Ca^{2+} entering through DHPRs can trigger CICR, the following features of CICR observed in the cotransfected CHO cells differ from those in cardiac myocytes and suggest that the spatial distance between the DHPRs and the RyRs is, on average, much larger in cotransfected CHO cells than in cardiac myocytes: (*1*) the activation rate of CICR is very slow (it takes 5–10 s to reach its peak), although the activation rate of Ca^{2+} current is similar to that of native cardiac myocytes. (*2*) Likewise, the onset of CICR appears to be slow and may develop after a substantial delay, since the secondary rise in $[Ca^{2+}]_i$ occasionally develops after a partial decay of the Ca^{2+} current component (cf. Fig. 7 *A*). Even though we cannot completely exclude the possibility that CICR may contribute to the rapid first component, the time to peak of the first component is usually several hundreds of milliseconds and is considerably slower than that of CaTs in cardiac myocytes (<40 ms with Fura-2). Also, the onset of CICR in native cardiac myocytes is extremely fast, occurring within 2–4 ms of depolarization (Cheng et al., 1994; Cannell et al., 1995). (*3*) The size of the Ca^{2+} release component is larger when the pulse duration is prolonged. It proved difficult to induce the CICR by pulses briefer than 100 ms, even though the Ca^{2+} current density is higher than that of cardiac myocytes. When the Ca^{2+} current density is lower than 20 pA/pF, the second component is rarely detected. By contrast, depolarizations as brief as 10 ms are sufficient to elicit maximal Ca^{2+} release in cardiac myocytes (Cleemann and Morad, 1991; Cannell et al., 1995). (*4*) When the CaTR is relatively large, CICR is all-or-none, whereas cardiac myocytes exhibit a graded CICR, despite a large gain (Cannell et al., 1987; Beuckelman and Wier, 1988; Wier et al., 1994). (*5*) When the concentration of Fura-2 was higher than 200 μM (data not shown), the CICR component was rarely observed, indicating that Ca^{2+} ions released from the RyRs when captured by moderate increases in buffering capacity with a fast and high affinity Ca^{2+} buffer, reduced the efficacy of CICR. In cardiac myocytes, even 10 mM EGTA fails to alter the effect of SR Ca^{2+} release on the Ca^{2+}-dependent inactivation of Ca^{2+} current (Sham et al., 1995*a*). (*6*) Tail current-induced Ca^{2+} transients, as occasionally observed in cardiac myocytes (Cannell et al., 1987; Cleemann and Morad, 1991; Cannell et al., 1995) were never observed in the cotransfected CHO cells.

Thus, the spatially averaged (global) increase in $[Ca^{2+}]_i$ rather than the local increase in $[Ca^{2+}]_i$ is likely to be involved in the initial triggering of Ca^{2+} release in the cotransfected CHO cells. It should be pointed out that the rate of increase in $[Ca^{2+}]_i$ due to CICR remained slow compared with that of cardiac myocytes even when optimizing conditions that are known to increase the sensitivity of the RyRs to Ca^{2+} (i.e., in the presence of 2 mM caffeine, low Mg^{2+} [0.35 mM] and high total ATP [8 mM]). This would suggest that the slowness of the Ca^{2+} release process in this preparation is not due to low Ca^{2+} sensitivity of the skeletal RyR isoform compared with that of the cardiac RyR isoform, but rather to the relative spatial distribution of the expressed receptors.

Skeletal-Type E-C Coupling Is Not Reconstituted in the Cotransfected CHO Cells

The spatial distance between the DHPRs (in the surface membrane) and the RyRs (in the membrane of internal Ca^{2+} stores) appears to be, on average, much larger in the transfected CHO cells than in cardiac myocytes, and hence, it is not surprising that there is no skeletal-type interaction between the DHPRs and the RyRs. The following evidence is in support of this view: (*1*) The CaT is strongly reduced and the second (CICR) component disappears in nominally Ca^{2+}-free saline. (*2*) The CaT exhibits a bell-shaped voltage dependence. (*3*) Repolarization fails to even partially curtail (or change the time derivative of) the depolarization-induced CaT. In other words, $[Ca^{2+}]_i$ continues to increase for several seconds following repolarization. (*4*) Repolarization fails to induce any dip in the caffeine-activated CaT, which suggests that activated RyRs are not influenced by the DHPR. In mammalian skeletal muscle, repolarization terminates caffeine-induced Ca^{2+} release (RISC phenomenon; Suda and Penner, 1994). Together, these results lead us to the conclusion that there is no direct interaction between the DHPRs and the RyRs in the transfected CHO cells (but see below).

Possible Indications of Direct Coupling between the DHPR and the RyR in Cotransfected CHO Cells

We cannot completely exclude the possibility that a small fraction of the RyRs might be directly coupled to the DHPRs and thereby contributes to voltage-gated Ca^{2+} release, resulting in a larger amount of Ca^{2+} release with a longer pulse (Brum et al., 1988*a*). Although our results suggest that Ca^{2+} release does not occur to any significant extent in the absence of $[Ca^{2+}]_o$, despite the caffeine-sensitive Ca^{2+} stores being sufficiently full (cf. Fig. 4 *C*), this may not unambiguously rule out some voltage-gated Ca^{2+} release component. One finding that might point towards a "facilitatory" role of depolarization on $[Ca^{2+}]_i$, that is not easily reconcilable with a simple CICR scheme, is that Ca^{2+} influx elicited by stronger depolarizations appears to release Ca^{2+} more efficiently than that by weak depolarizations (cf. Fig. 4 *D*). Also, one should recall that when the chimeric DHPR (cytoplasmic loop between repeats II and III is of skeletal origin and the remainder is cardiac) was expressed in dysgenic myotubes, voltage-gated Ca^{2+} release occurred more efficiently in the presence of $[Ca^{2+}]_o$ than in the absence of $[Ca^{2+}]_o$ (Tanabe et al., 1990). Furthermore, it is possible that the caffeine-sensitive pools that contribute to direct coupling of both receptors are located very close to the surface membrane and thus are easily emptied upon removal of extracellular Ca^{2+}. Because the total capacity of these pools may be small compared to other caffeine-sensitive pools, caffeine might still be able to induce Ca^{2+} release from the pools which are located far away from the surface membrane.

The results presented in this study are basically in accordance with structural features of the same transformant (Takekura et al., 1995*b*), in which no junctions are formed. Recently, Takekura et al. (1995*a*) have shown in "dyspedic" myotubes that even in the absence of feet (corresponding to the RyRs), junctions are formed between the T-tubule membranes and the SR membranes, although the length of the junctions are shorter than those observed in normal muscle, probably because of the lack of the feet structures. This would suggest that proteins other than the DHPR and the RyR are necessary for the initial forming of junctions between the T-tubule and the SR membranes. CHO cells may lack the necessary proteins for linking the surface membrane to ER membranes (Takekura et al., 1995*a*,*b*). Such proteins may also be involved in diadic junctions in cardiac muscle to accomplish tight control of SR Ca^{2+} release by relatively small Ca^{2+} entry through the DHPR Ca^{2+} channels.

We are grateful to the late Dr. S. Numa for support and constant encouragement during the early stage of this project, Dr. T. Tanabe for the cardiac-skeletal DHPR chimera, Drs. V. Flockerzi and F. Hofmann for β and γ subunits of the DHPR, Dr. K.P. Campbell for antibody to the skeletal DHPR. We also thank Dr. E. Neher for constant encouragement, support, and comments on the manuscript, Dr. S.H. Heinemann for help with gating current measurement, Drs. K.G. Beam, A. Korotzer, and N.M. Losenzon at Colorado State University for critical reading and comments on the manuscript, Drs. K. Imoto and J. Nakai at National Institute for Physiological Sciences (Japan) for helpful discussions and comments on the manuscript, Dr. Y. Hakamata at Kyoto University for stimulating discussions during the early stage of this project. Finally, we thank Frauke Friedlein and Michael Pilot for excellent technical assistance.

This work was supported by the following institutions: Deutsche Forschungsgemeinschaft, Sonderforschungsbereich 236, Hermann-und Lilly-Schilling-Stiftung to R. Penner; The Ministry of Education, Science and Culture (Japan) and The Japan Heart Foundation (I.B.M.) to H. Takeshima. N. Suda was supported by Ciba-Geigy Foundation for the Promotion of Science (Japan) and a grant from the Max-Planck-Gesellschaft. The manuscript was written while N. Suda received a grant from the Human Frontier Science Program.

Original version received 29 October 1996 and accepted version received 25 February 1997.

REFERENCES

Adams, B.A., T. Tanabe, A. Mikami, S. Numa, and K.G. Beam. 1990. Intramembrane charge movement restored in dysgenic skeletal muscle by injection of dihydropyridine receptor cDNA. *Nature (Lond.).* 346:569–572.

Barcenas-Ruiz, L., and W.G. Wier. 1987. Voltage dependence of intracellular [Ca^{2+}] transients in guinea pig ventricular myocytes. *Circ. Res.* 61:148–154.

Beuckelman, D.J., and W.G. Wier. 1988. Mechanism of release of calcium from sarcoplasmic reticulum of guinea-pig cardiac cells. *J. Physiol.* 405:233–255.

Block, B.A., T. Imagawa, K.P. Campbell, and C. Franzini-Armstrong. 1988. Structural evidence for direct interaction between the molecular components of the transverse tubule/sarcoplasmic reticulum junction in skeletal muscle. *J. Cell Biol.* 107:2587–2600.

Brandt, N., and A. Basset. 1986. Separation of dihydropyridine binding sites from cardiac junctional sarcoplasmic reticulum. *Arch. Biochem. Biophys.* 244:872–875.

Brandt, N.R., A.H. Caswell, S.R. Wen, and J.A. Talvenheimo. 1990. Molecular interaction of the junctional foot protein and dihydropyridine receptor in skeletal muscle triads. *J. Memb. Biol.* 113: 237–251.

Brum, G., R. Fitts, G. Pizarro, and E. Rios. 1988*a*. Voltage sensors of the frog skeletal muscle membrane require calcium to function in excitation-contraction coupling. *J. Physiol.* 398:475–505.

Brum, G., E. Rios, and E. Stephani. 1988*b*. Effects of extracellular calcium on the calcium movements of excitation-contraction coupling in skeletal muscle fibres. (Appendix by Brum, E., E. Rios, and M.F. Schneider) *J. Physiol.* 398:441–473.

Callewaert, G., L. Cleemann, and M. Morad. 1988. Epinephrine enhances Ca^{2+} current-regulated Ca^{2+} release and Ca^{2+} reuptake in rat ventricular myocytes. *Proc. Natl. Acad. Sci. USA.* 85:2009–2013.

Cannell, M.B., J.R. Berlin, and W.J. Lederer. 1987. Effect of membrane potential change on the calcium transient in single rat cardiac muscle cells. *Science (Wash. DC).* 238:1419–1423.

Cannell, M.B., H. Cheng, and W.J. Lederer. 1995. The control of calcium release in heart muscle. *Science (Wash. DC).* 268:1045–1049.

Chandler, W.K., R.F. Rakowski, and M.F. Schneider. 1976. Effect of glycerol treatment and maintained depolarization on charge movement in skeletal muscle. *J. Physiol.* 254:285–316.

Cheng, H., M.B. Cannell, and W.J. Lederer. 1994. Propagation of excitation-contraction coupling into ventricular myocytes. *Pflügers Arch.* 428:415–417.

Cleemann, L., and M. Morad. 1991. Role of Ca^{2+} channel in cardiac excitation-contraction coupling in the rat: evidence from Ca^{2+} transients and contraction. *J. Physiol.* 432:283–312.

Fabiato, A. 1985. Time and calcium dependence of activation and inactivation of calcium-induced release of calcium from the sarcoplasmic reticulum of a skinned canine cardiac purkinje cell. *J. Gen. Physiol.* 85:247–289.

Franzini-Armstrong, C., and A.O. Jorgensen. 1994. Structure and development of E-C coupling units in skeletal muscle. *Ann. Rev. Physiol.* 56:509–534.

Györke, S., and M. Fill. 1993. Ryanodine receptor adaptation: control mechanism of Ca^{2+}-induced Ca^{2+} release in heart. *Science (Wash. DC).* 260:807–809.

Harrison, S.M., and D.M. Bers. 1987. The effect of temperature and ionic strength on the apparent Ca-affinity of EGTA and the analogous Ca-chelators BAPTA and dibromo-BAPTA. *Biochim. Biophys. Acta.* 925:133–143.

Lopez-Lopez, J.R., P.S. Shacklock, C.W. Balke, and W.G. Wier. 1995. Local calcium transients triggered by single L-type calcium channel currents in cardiac cells. *Science (Wash. DC).* 268:1042–1045.

Marty, I., M. Robert, K. Villaz, Y. Dejongh, W. Lai, A. Catterall, and M. Ronjat. 1994. Biochemical evidence for a complex involving dihydropyridine receptor and ryanodine receptor in triad junctions of skeletal muscle. *Proc. Natl. Acad. Sci. USA.* 91:2270–2274.

Meissner, G. 1994. Ryanodine receptor/Ca^{2+} release channels and their regulation by endogenous effectors. *Ann. Rev. Physiol.* 56: 485–508.

Näbauer, M., G. Callewaert, L. Cleemann, and M. Morad. 1989. Regulation of calcium release is gated by calcium current, not gating charge, in cardiac myocytes. *Science (Wash. DC).* 244:800–803.

Nakai, J., R.T. Dirksen, H.T. Nguyen, I.N. Pessah, K.G. Beam, and P.D. Allen. 1996. Enhanced dihydropyridine receptor channel activity in the presence of ryanodine receptor. *Nature (Lond.).* 380:72–75.

Penner, R., E. Neher, H. Takeshima, S. Nishimura, and S. Numa. 1989. Functional expression of the calcium release channel from skeletal muscle ryanodine receptor cDNA. *FEBS Lett.* 259:217–221.

Pizarro G., R. Fitts, I. Uribe, and E. Rios. 1989. The voltage sensors of excitation-contraction coupling in skeletal muscle. *J. Gen. Physiol.* 94:405–428.

Rios, E., and G. Brum. 1987. Involvement of dihydropyridine receptors in excitation-contraction coupling. *Nature (Lond.).* 325:717–720.

Rios, E., M. Karhanek, J. Ma, and A. Gonzalez. 1993. An allosteric model of the molecular interactions of excitation-contraction coupling in skeletal muscle. *J. Gen. Physiol.* 102:449–481.

Rios, E., and G. Pizarro. 1991. Voltage sensor of excitation-contraction coupling in skeletal muscle. *Physiol. Rev.* 71:849–908.

Rose, W.C., C.W. Balke, W.G. Wier, and E. Marban. 1992. Macroscopic and unitary properties of physiological ion flux through L-type Ca^{2+} channels in guinea-pig heart cells. *J. Physiol.* 456:267–284.

Sham, J.S.K., L. Cleemann, and M. Morad. 1995*a*. Functional coupling of Ca^{2+} channels and ryanodine receptors in cardiac myocytes. *Proc. Natl. Acad. Sci. USA.* 92:121–125.

Sham, J.S.K., S.N. Hatem, and M. Morad. 1995*b*. Species differences in the activity of the Na^{+}-Ca^{2+} exchanger in mammalian cardiac myocytes. *J. Physiol.* 488:623–631.

Stern, M.D. 1992. Theory of excitation-contraction coupling in cardiac muscle. *Biophys. J.* 63:497–517.

Suda, N., M. Bödding, A. Fleig, D. Franzius, M. Hoth, S. Nishimura, K. Imoto, H. Takeshima, and R. Penner. 1996. Slow calcium-induced calcium release (CICR) in chinese hamster ovary (CHO)

cells expressing skeletal ryanodine receptor (RyR) and chimaeric dihydropyridine receptor (DHPR). *Biophys. J.* 70:A387. (Abstr.)

Suda, N., and R. Penner. 1994. Membrane repolarization stops caffeine-induced Ca^{2+} release in skeletal muscle. *Proc. Natl. Acad. Sci. USA*. 91:5725–5729.

Takekura, H., M. Nishi, T. Noda, H. Takeshima, and C. Franzini-Armstrong 1995*a*. Abnormal junctions between surface membrane and sarcoplasmic reticulum in skeletal muscle with a mutation targeted to the ryanodine receptor. *Proc. Natl. Acad. Sci. USA*. 92:3381–3385.

Takekura, H., H. Takeshima, S. Nishimura, M. Takahashi, T. Tanabe, V. Flockerzi, F. Hofmann, and C. Franzini-Armstrong. 1995*b*. Co-expression in CHO cells of two muscle proteins involved in excitation-contraction coupling. *J. Muscle. Res. Cell Motil.* 16:465–480.

Takeshima, H., M. Iino, H. Takekura, M. Nishi, J. Kuno, O. Minowa, H. Takano, and T. Noda. 1994. Excitation-contraction uncoupling and muscular degeneration in mice lacking functional skeletal muscle ryanodine-receptor gene. *Nature (Lond.)*. 369: 556–559.

Takeshima, H., S. Nishimura, T. Matsumoto, H. Ishida, K. Kanagawa, N. Minamino, H. Matsuo, M. Ueda, M. Hanaoka, T. Hirose, and S. Numa. 1989. Primary structure and expression from complementary DNA of skeletal muscle ryanodine receptor. *Nature (Lond.)*. 339:439–445.

Tanabe, T., K.G. Beam, B.A. Adams, T. Niidome, and S. Numa. 1990. Regions of the skeletal muscle dihydropyridine receptor critical for excitation-contraction coupling. *Nature (Lond.)*. 346: 567–569.

Tanabe T., K.G. Beam, J.A. Powell, and S. Numa. 1988. Restoration of excitation-contraction coupling and slow calcium current in dysgenic muscle by dihydropyridine receptor complementary DNA. *Nature (Lond.)*. 336:134–139.

Valdivia, H.H, J.H. Kaplan, G.C.R. Ellis-Davies, and W.J. Lederer. 1995. Rapid adaptation of cardiac ryanodine receptors: modulation by Mg^{2+} and phosphorylation. *Science (Wash. DC.)* 267:1997–2000.

Wier, W.G., T.M. Egan, J.R. Lopez-Lopez, and C.W. Balke. 1994. Local control of excitation-contraction coupling in rat heart cells. *J. Physiol.* 474:463–471.

Yasui, K., P. Palade, and S. Györke. 1994. Negative control mechanism with features of adaptation controls Ca^{2+} release in cardiac myocytes. *Biophys. J.* 67:457–460.